Cancer Chemother Pharmacol (2005) 55: 21–32
DOI 10.1007/s00280-004-0865-3

ORIGINAL ARTICLE

**Julie L. Eiseman · Jing Lan · Theodore F. Lagattuta
Deborah R. Hamburger · Erin Joseph
Joseph M. Covey · Merrill J. Egorin**

Pharmacokinetics and pharmacodynamics of 17-demethoxy 17-[[(2-dimethylamino)ethyl]amino]geldanamycin (17DMAG, NSC 707545) in C.B-17 SCID mice bearing MDA-MB-231 human breast cancer xenografts

Received: 4 February 2004 / Accepted: 25 May 2004 / Published online: 27 August 2004

Abstract *Purpose*: 17-demethoxy 17-[[(2-dimethylamino)ethyl]amino]geldanamycin (17DMAG, NSC 707545) is a water-soluble analogue of 17-(allylamino)-17-demethoxygeldanamycin (17AAG), a compound currently in clinical trials. These preclinical studies: (1) characterized 17DMAG concentrations in plasma, normal tissues, and tumor after i.v. delivery to mice; and (2) correlated tumor and normal tissue 17DMAG concentrations with alterations in heat shock protein 90 (HSP90) and selected HSP90-chaperoned proteins. *Methods*: At specified times after i.v. administration of 75 mg/kg 17DMAG, SCID mice bearing s.c. MDA-MB-231 human breast xenografts were killed and plasma and tissues were retained. 17DMAG concentrations were determined by HPLC. Raf-1, heat shock protein 70 (HSP70), and HSP90 in tissues were determined by Western blotting. *Results*: Peak plasma 17DMAG concentration was 15.4 ± 1.4 μg/ml. The area under the plasma 17DMAG concentration versus time curve was 1072 μg/ml min, corresponding to a total body clearance of 70 ml/kg/min. Peak 17DMAG concentrations in liver (118.8 ± 5.7 μg/g), kidney (122.9 ± 10.6 μg/g), heart (81.3 ± 8.1 μg/g), and lung (110.6 ± 25.4 μg/g) occurred at 5–10 min, while peak concentrations in spleen (70.6 ± 9.6 μg/g) and tumor (9.0 ± 1.0 μg/g) occurred at 30–45 min. At 48 h, 17DMAG was detectable in tumor but not in any normal tissue. Raf-1 in tumors of 17DMAG-treated mice killed at 4, 7, 24 and 48 h was about 20% lower than in tumors from vehicle-treated mice. HSP90 and HSP70 in tumors of 17DMAG-treated animals were significantly lower than in tumors of control animals at 4, 7, and 24 h. Hepatic Raf-1 was decreased by more than 60% at all times after 17DMAG treatment; however, hepatic HSP90 was not affected. HSP70 was undetectable in livers of vehicle-treated mice or mice killed at 2 or 4 h after 17DMAG treatment, but was detected in livers at 7, 24 and 48 h. 17DMAG did not affect renal Raf-1. In contrast, renal HSP70 and HSP90 were decreased by more than 50% at 2 and 4 h after 17DMAG treatment. Renal HSP70 increased approximately twofold above that in kidneys from vehicle-treated control mice at 7 and 24 h, while HSP90 relative protein concentration was no different from that in controls. *Conclusions*: Plasma pharmacokinetics of 17DMAG in tumor-bearing mice were similar to those previously reported in nontumor-bearing mice. 17DMAG was distributed widely to tissues but was retained for longer in tumors than normal tissues. Raf-1, HSP90, and HSP70 were altered to different degrees in tumors, livers, and kidneys of 17DMAG-treated animals. These data illustrate the complex nature of the biological responses to 17DMAG.

This work was supported by contract NO1-CM07106 and Grant 2P30 CA47904, awarded by the National Cancer Institute.

J. L. Eiseman · J. Lan · M. J. Egorin
Department of Pharmacology,
University of Pittsburgh School of Medicine,
Pittsburgh, PA 15213, USA

J. L. Eiseman (✉) · J. Lan · T. F. Lagattuta
D. R. Hamburger · E. Joseph · M. J. Egorin
Molecular Therapeutics/Drug Discovery Program,
University of Pittsburgh Cancer Institute,
G27b Hillman Research Pavilion, 5117 Centre Ave.,
Pittsburgh, PA 15213, USA
E-mail: eisemanj@msx.upmc.edu
Tel.: +1-412-6233239
Fax: +1-412-6231212

J. M. Covey
Toxicology and Pharmacology Branch,
Developmental Therapeutics Program,
Division of Cancer Treatment and Diagnosis,
National Cancer Institute, Bethesda,
MD 20892, USA

M. J. Egorin
Division of Hematology/Oncology, Department of Medicine,
University of Pittsburgh School of Medicine,
Pittsburgh, PA 15213, USA

Keywords Geldanamycin · Heat shock proteins · Pharmacokinetics · Pharmacodynamics

Introduction

17-Demethoxy 17-[[(2-dimethylamino)ethyl]amino]geldanamycin (17DMAG, NSC 707545) [28, 58, 59] is an analogue of geldanamycin [17, 52, 63, 69] and 17-(allylamino)-17-demethoxygeldanamycin (17AAG) [18, 20, 22], the latter of which is currently in clinical trials [7, 13, 24, 61, 67] (Fig. 1). The antiproliferative activity of geldanamycin and 17AAG is related to their ability to bind specifically to heat shock protein 90 (HSP90) [26, 45, 47, 49, 51, 62] and its homologue GRP94, destabilize HSP90-oncoprotein heterocomplexes, and thereby deplete oncoproteins such as $p185^{erbB2}$, mutant p53, Raf-1, and other proteins that are clients of HSP90 [2–5, 8, 9, 12, 31, 33, 34, 37, 39, 42, 43, 54, 56, 60, 66, 68].

Fig. 1 Structures of geldanamycin, 17AAG, 17AG, 17DMAG, and previously known metabolites of 17AAG

Although 17AAG, which is currently undergoing extensive clinical evaluation [7, 13, 24, 61, 67], was developed as part of an effort to develop novel, potent, and selective inhibitors of HSP90 that are useful antitumor agents [4, 25, 35, 40, 41, 48, 53, 64], it has several drawbacks, including formulation in a relatively complex vehicle and metabolism by CYP3A to potentially toxic metabolites [18, 20]. Thus, there are ongoing efforts to develop additional geldanamycin analogues that have advantages over 17AAG. One of these, 17DMAG [21, 23, 28, 58, 59], is about to enter clinical trials.

We have extended earlier studies, in which the plasma pharmacokinetics and tissue distribution of 17DMAG were determined in normal CD_2F_1 mice [21], by characterizing the pharmacokinetics and pharmacodynamics of 17DMAG in SCID mice bearing xenografts of the human estrogen receptor-negative breast cancer, MDA-MB-231. The objectives were to: (1) determine if the plasma pharmacokinetics and tissue distribution of 17DMAG were similar in tumor-bearing and nontumor-bearing mice; (2) define the concentrations and time

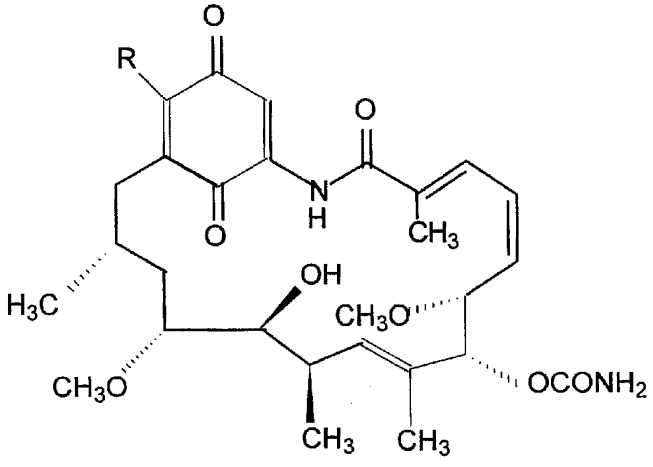

Compound		R	Molecular Weight
Geldanamycin		CH_30	560
17-(allylamino)-17-demethoxygeldanamycin	**17AAG**	CH_2=CH-CH_2-NH	585
17-(amino)-17-demethoxygeldanamycin	**17AG**	NH_2	545
Epoxide Metabolite		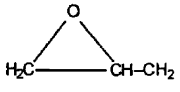	601
Diol Metabolite		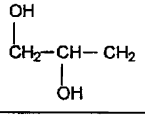	619
17-(dimethylaminoethylamino)-17-demethoxygeldanamycin	**17DMAG**	$(CH_3)_2$NH-CH-CH_2-NH	617

course of 17DMAG in tumor tissue; and (3) investigate whether treatment with 17DMAG resulted in alterations in relative protein concentrations of HSP90 and selected HSP90 client proteins in tumor and normal tissues.

Materials and methods

Reagents

Alpha-naphthoflavone was purchased from Aldrich Chemicals (Milwaukee, Wis.). Sodium pyrophosphate, sodium vanadate, sodium fluoride, aprotinin, leupeptin, pepstatin, microcystin and Nonidet P40 were purchased from Sigma Chemical Company (St Louis, Mo.). Tris-glycine-SDS buffer, SDS 4–15% gel packs, PVDF membranes, goat anti-rabbit IgG-HPR-conjugated antibody or rabbit anti-mouse IgG-HPR-conjugated antibody, prestained protein markers, and a protein assay kit were purchased from BioRad (Hercules, Calif.). Antibodies against HSP70 and HSP90 (SPA-810 and SPA-830) were purchased from StressGen Biotechnology Corporation (Victoria, Canada). Antibodies against Raf-1 (sc-133) and β-actin (clone AC-15) were purchased from Santa Cruz Biotechnology (Santa Cruz, Calif.) and Sigma Chemical Company, respectively. A Western blot chemiluminescence (ECL) detection system was purchased from NEN Life Science Products (Boston, Mass.).

Drugs

17DMAG, 17AAG, and 17AG were supplied by the Developmental Therapeutics Program, National Cancer Institute (Bethesda, Md.) and were stored in the dark at 4–8°C until use. Dosing solutions of 17DMAG were prepared at 5.0 mg/ml in sterile 5% dextrose-in-water (D5W). 17DMAG dosing solutions were freshly prepared on the morning of each study.

Mice

Specific-pathogen-free adult female SCID mice (5–6 weeks of age) were obtained from the animal program administered by the Biological Testing Branch of the National Cancer Institute. Mice were handled in accordance with the Guide for the Care and Use of Laboratory Animals (National Research Council, 1996) and on a protocol approved by the Institutional Animal Care and Use Committee of the University of Pittsburgh. Mice were given at least 1 week to acclimate to the animal facility before they were studied. To minimize exogenous infection, mice were maintained in sterile microisolator cages. Ventilation and air flow in the animal facility were set to 12 changes per hour. Room temperature was regulated at 72 ± 2°F, and the rooms were kept on automatic 12-h light/dark cycles. Mice received Prolab ISOPRO RMH 3000, Irradiated Lab Diet (PMI Nutrition International, Brentwood, Mo.) and sterile water ad libitum. However, on the evening prior to study, food was removed at approximately 6 p.m. and withheld until 4 h after dosing on the next day. Sentinel mice, housed in 20% dirty bedding from study mice, remained murine antibody profile-negative using Assessment + (Charles River Laboratories, Wilmington, Mass.), indicating that the study mice were specific-pathogen-free.

Tumor cell lines

MDA-MB-231 human breast cancer cells were obtained from ATCC (Manassas, Va.) and expanded in culture in RPMI 1640 medium (Gibco, InVitrogen Corporation, Carlsbad, Calif.) supplemented with 10% fetal bovine serum (Biofluids, Rockville, Md.) and 10 μg/ml gentamicin (Gibco, InVitrogen). Cells were maintained at 37°C in an incubator under an atmosphere of 95% air/5% CO_2 at 95% humidity.

For in vitro studies, MDA-MB-231 cells were plated into 30-mm culture dishes at a concentration of 5×10^5 cells per dish. After 24 h, 100 μl 17DMAG in 5% D5W or 100 μl D5W was added to the culture medium, and the dishes were gently mixed. The final concentrations of 17DMAG in the culture dishes were 20 or 100 n*M*. At 7 or 24 h after the addition of 17DMAG in D5W or 24 h after the addition of D5W, the medium was removed, and the cells were rinsed with Hanks balanced salt solution. Cells from three culture dishes per treatment at each time point were harvested using a cell scraper, transferred by pipette to a microcentrifuge tube and centrifuged at 13,000 *g* for 2 min. The resulting supernatant was discarded, and the cell pellets were lysed using lysing buffer. The relative protein concentrations of HSP90, HSP70 and Raf-1 in cell lysates were determined by Western blot analysis as described below.

Before implantation into study animals, cells (5×10^6 cells/mouse) were injected s.c. into the right flanks of passage SCID mice. Tumor volumes were calculated twice weekly using the formula, vol (mm^3) = $L\times W^2/2$, and length (L, mm) and width (W, mm) were measured using a digital caliper. When the tumors in the passage mice reached approximately 500–1000 mm^3, the mice were killed, and the tumors were removed using sterile technique. Tumors were cut into approximately 25-mg fragments, and the fragments were placed in sterile medium until s.c. implantation on the right flanks of the study mice. When tumor volumes were greater than 200 mm^3, the study mice were stratified into groups ($n = 3$) by body weight and tumor volume so that all groups were similar based on results of ANOVA (Minitab, State College, Pa.).

Dosing

17DMAG (0.015 ml/g exact body weight) was administered as an i.v. bolus at 75 mg/kg through a 27-gauge

needle and into a lateral tail vein. Vehicle-treated mice received D5W at 0.015 ml/g exact body weight. 17DMAG concentrations in dosing solutions were confirmed with the HPLC assay described below.

Sampling

Three mice were killed by CO_2 inhalation, and blood was collected by cardiac puncture using heparinized syringes at the following times after dosing: 5, 10, 15, 30, 45, 60, 120, 180, 240, 360, 420, 1140, 1440, and 2880 min or 5 min after the administration of vehicle. Blood was transferred to microcentrifuge tubes and stored on ice until centrifuged at 13,000 *g* for 4 min to obtain plasma and red blood cells (RBCs). Livers, kidneys, hearts, lungs, spleens and tumors were rapidly dissected, placed on ice, weighed, transferred to cryovials, and snap-frozen in liquid nitrogen. RBCs, plasma and tissues were stored at −70°C until analysis by HPLC as described below. Three additional mice were killed at 120, 240, 420, 1440, and 2880 min after i.v. dosing with 75 mg/kg 17DMAG or at 5, 1440 and 2880 min after i.v. administration of vehicle. The tissues from these mice were handled as described above, except the tissue samples were used for Western blot analysis of HSP70, HSP90, and Raf-1.

HPLC analysis

Plasma and tissue concentrations of 17DMAG were determined using a previously published HPLC method [20, 21]. Because there was a remote possibility that 17AG could be a metabolite of 17DMAG [21], standard curves were prepared for both 17DMAG and 17AG. Internal standard (5 µl of 200 µg/ml 17AAG in acetonitrile) was added to each plasma sample, which were extracted directly. Tissues were thawed on ice and homogenized in three volumes of phosphate-buffered saline, pH 7.4 (Biofluids, Rockville, Md.), and internal standard was added prior to extraction.

The HPLC system consisted of a Waters 717 autosampler and a Waters 600E system controller and solvent delivery system fitted with a Waters Novapak C18 guard column and a Waters Novapak C18 column (5 µm, id 3.9×150 mm; Waters Associates, Milford, Mass.). A gradient mobile phase consisting of acetonitrile/25 m*M* sodium phosphate, pH 3.0, with 10 m*M* triethylamine (65:35, v/v) was pumped at 1 ml/min. Column eluate was monitored at 330 nm with a Spectroflow 757 absorbance detector (ABI Analytical, Kratos Division, Ramsey, N.Y.), and detector output was processed with Chrom Perfect software (Justice Innovations, Denville, N.J.) so as to integrate the areas under the 17DMAG and internal standard peaks. Concentrations of 17DMAG were determined by calculating the ratio of the area of the 17DMAG peak to that of internal standard in the sample and comparison of that ratio to a concomitantly performed standard curve that had been prepared in the appropriate biological matrix. Specific details regarding the quantitative performance of this assay in our laboratory have been published previously [21].

Pharmacokinetic analysis

The time-course of plasma 17DMAG concentrations was analyzed by both noncompartmental and compartmental methods. The area under the concentration versus time curve (AUC) and $t_{1/2}$ were estimated by noncompartmental analysis using the LaGrange function [70], as implemented by the computer program LAGRAN [50]. Total body clearance (CL_{tb}) was calculated from the equation:

$$CL_{tb} = \text{Dose}/\text{AUC},$$

and steady-state volume of distribution (V_{dss}) was calculated as follows:

$$V_{dss} = \text{Dose} \times \left(\text{AUMC}/\text{AUC}^2\right),$$

where AUMC is the area under the moment curve.

Tissue AUCs were also calculated using the LaGrange function.

Compartmental modeling using mean concentrations of 17DMAG detected in plasma was performed with the program ADAPT II [16], using maximum likelihood estimation. Two- and three-compartment open linear models were fitted to the data, and model discrimination was based on Akaike's information criteria (AIC), calculated as:

$$\text{AIC} = 2p + n(\ln \text{WSSR})$$

where p represents the number of parameters, n is the number of observations and WSSR is the weighted sum of squares residuals [1].

Western blots

Tissues were thawed on ice and homogenized using an Omni Tissuemizer (Omni International, Westbury, Ct.) in ten volumes of ice-cold lysing extraction buffer. The lysing extraction buffer consisted of: 50 m*M* Tris-HCl, pH 7.9, 2 m*M* EDTA, 100 m*M* NaCl, and 1% Nonidet P40. Freshly prepared protease inhibitors were added just prior to homogenization and included 10 m*M* NaF, 10 m*M* sodium vanadate, 1 µg/ml pepstatin, 10 µg/ml aprotinin, 5 µg/ml leupeptin, 5 m*M* PMSF, 0.1 µ*M* microcystin, and 5 m*M* Na pyrophosphate. After homogenization, the samples were centrifuged for 10 min at 13,000 *g*. The cold supernatant was divided into aliquots, transferred to cryovials, and stored at −70°C until analysis. Tissue homogenate protein concentrations were determined using the Bio-Rad protein assay kit and bovine serum albumin standard curves.

Protein concentrations in samples were adjusted so that 20–30 μg of protein was loaded into each well. Samples were diluted with 3×, modified Laemmli sample buffer (Bio-Rad), which contained 0.4 *M* Tris-HCl, pH 6.8, 8% SDS, 39% glycerol, 0.04% bromophenol blue, and 0.4 *M* dithiothreitol. Sample protein or protein standards (20 μl) were loaded onto 4–15% SDS gradient gels. Proteins were separated by electrophoresis and then electrotransferred to PVDF membranes and blotted with antibodies against Raf-1, HSP90 and HSP70. The membranes were also blotted with an antibody against *β*-actin, and *β*-actin relative protein concentration was used as a loading control. Blots were developed using an ECL detection system. Immunoreactivity signals were quantified by densitometry with UN-SCAN-IT software (Silk Scientific, Orem, Utah). The pixels for each band were normalized to the pixels of the corresponding *β*-actin band. All values for each marker were then normalized to the control markers. This was done by dividing the values for each marker by the values obtained for each marker in the control animals, and the mean for each of the treated groups was calculated. No differences in detection by the Western blots were observed when antibodies were used separately or when they were combined, and the immunoreactivity signals were linear over a protein range of 4–32 μg loaded on the gel.

Results

Pharmacokinetic studies

After an i.v. dose of 75 mg/kg, "peak" plasma 17DMAG concentrations were measured at 5 min after injection and were 15.4 ± 1.4 μg/ml (Table 1). Thereafter, plasma 17DMAG concentrations declined with a half-life ($t_{1/2}$) of 32–55 min and in a manner best fit by a two-compartment open linear model (Fig. 2a), so that by 420 min, they were below the lower limit of quantitation of the HPLC assay used (Table 1, Fig. 2a). When calculated with noncompartmental methods, the plasma AUC was 1072 μg/ml min, corresponding to a CL_{tb} of

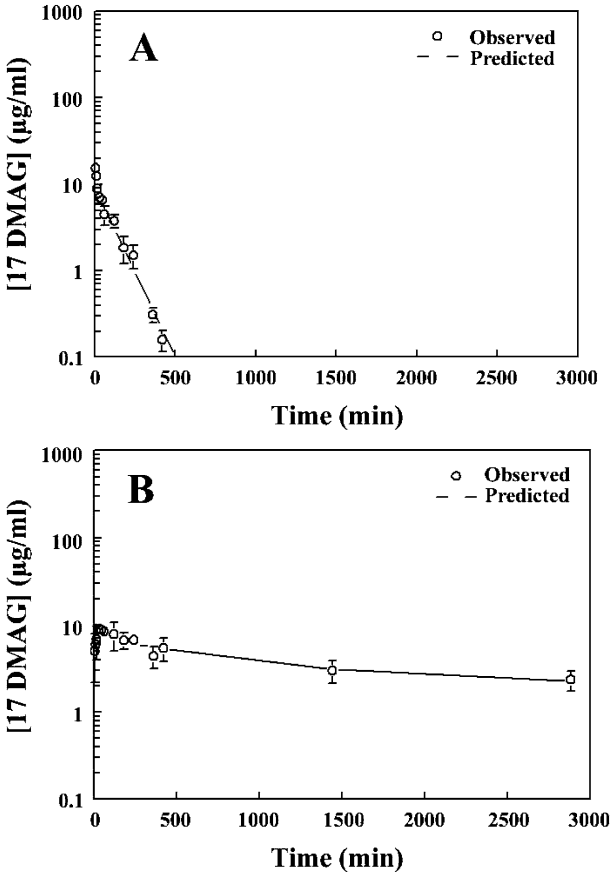

Fig. 2 Concentrations of 17DMAG detected in (**a**) plasma and in (**b**) tumor of C.B-17 SCID female mice bearing MDA-MB-231 tumor and given a 75 mg/kg i.v. dose of 17DMAG. The data points (*circles*) represent the mean of three samples at each time point, and error bars represent ± SD. *Lines* represent the predicted data by compartmental modeling

Table 1 Concentrations and AUCs of 17DMAG in plasma and tissues of C.B-17 SCID mice bearing MDA-MB-231 tumors and injected i.v. with a 75 mg/kg dose of 17DMAG. Each value is the mean ± SD of three samples (*ND* not detected)

Time (min)	Plasma (μg/ml)	Liver (μg/g)	Kidney (μg/g)	Lung (μg/g)	Heart (μg/g)	Spleen (μg/g)	Tumor (μg/g)
5	15.4 ± 1.4[1]	102.9 ± 47.5	109.4 ± 29.2	110.6 ± 25.4	81.3 ± 8.1	28.2 ± 16.4	5.0 ± 2.8
10	12.4 ± 0.2	118.8 ± 5.7	122.9 ± 10.6	97.6 ± 15.1	67.6 ± 23.9	46.8 ± 7.8	6.0 ± 0.4
15	8.9 ± 0.6	103.2 ± 11.0	103.0 ± 10.2	76.3 ± 11.6	46.5 ± 3.8	66.1 ± 10.2	6.9 ± 2.9
30	7.0 ± 1.2	82.7 ± 7.2	87.4 ± 2.2	68.9 ± 1.8	36.8 ± 10.4	63.5 ± 14.1	9.0 ± 1.0
45	6.6 ± 0.5	84.6 ± 20.2	75.9 ± 4.3	56.1 ± 1.1	23.6 ± 1.9	70.6 ± 9.6	8.8 ± 1.3
60	4.5 ± 1.1	64.9 ± 16.9	63.7 ± 26.3	38.7 ± 14.4	17.0 ± 8.7	49.3 ± 21.3	8.5 ± 0.4
120	3.8 ± 0.7	41.7 ± 9.2	41.7 ± 11.6	26.2 ± 4.0	11.5 ± 4.0	37.4 ± 10.6	7.8 ± 2.8
180	1.8 ± 0.7	30.3 ± 9.0	25.8 ± 9.1	13.0 ± 3.2	5.1 ± 1.5	18.8 ± 5.2	6.7 ± 1.4
240	1.5 ± 0.5	21.6 ± 2.6	ND	10.9 ± 2.1	3.9 ± 0.9	17.1 ± 3.7	6.7 ± 0.7
360	0.3 ± 0.1	6.4 ± 1.9	4.0 ± 1.8	3.4 ± 0.9	0.5 ± 0.4	5.9 ± 1.8	4.4 ± 1.3
420	0.2 ± 0.0	8.1 ± 1.0	3.5 ± 1.0	3.3 ± 0.1	0.3 ± 0.6	5.9 ± 0.8	5.4 ± 1.6
1440	ND[2]	2.1 ± 1.9	0.4 ± 0.4	0.4 ± 0.6	ND	0.8 ± 1.0	3.0 ± 0.8
2880	ND	ND	ND	ND	ND	ND	2.4 ± 0.6
$AUC_{0-\infty}$(μg min/ml or μg min/g)	1,072	25,693	13,520	10,552	3,748	14,569	19,876

Table 2 Compartmental and noncompartmental pharmacokinetic analyses of plasma 17DMAG concentration-versus-time data associated with administration of 17DMAG (75 mg/kg i.v.) to C.B-17 SCID mice bearing MDA-MB-231 xenografts. Compartmental modeling was performed using the program Adapt II (k_{12} transfer rate constant from the central compartment to the peripheral compartment, k_{21} transfer constant from the peripheral compartment back to the central compartment, k_{10} elimination rate constant from the central compartment, V_c volume of the central compartment)

Analysis	k_{12} (min^{-1})	k_{21} (min^{-1})	k_{10} (min^{-1})	$t_{1/2}$ (min)	V_c (ml/kg)	$AUC_{0-\infty}$ (μg min/ml)	V_{dss} (ml/kg)	CL_{tb} (ml/min/kg)
Compartmental	0.0813	0.0646	0.0220	32	3044	1119	5797	67
Noncompartmental				55		1072	7701	70

70 ml/min/kg. Very similar values for AUC and CL_{tb} were obtained when a two-compartment open linear model was fitted to the plasma concentration versus time data (Tables 1 and 2). Other pharmacokinetic parameters related to noncompartmental and compartmental analyses of plasma 17DMAG concentration versus time data are displayed in Table 2.

After i.v. administration, 17DMAG was widely distributed to tissues (Table 1). The highest tissue concentrations of 17DMAG were observed in liver, kidney, and lung, with lower concentrations being present in heart, spleen, and tumor at the early time points. 17DMAG concentrations in liver, kidney, and lung peaked at 5 min and were approximately eight- to tenfold higher than the 17DMAG concentrations observed in plasma at that time. Peak spleen 17DMAG concentrations did not occur until 45 min after 17DMAG administration. Although 17DMAG concentrations in all tissues declined with time, 17DMAG was detected in all tissues for at least 7 h after drug delivery and persisted in liver, spleen, kidney, and lung for 24 h. When expressed as AUC, the exposure of all the tissues to 17DMAG was greater than that of plasma (Table 1). 17DMAG concentrations in tumor peaked later and persisted longer than in normal tissues. Specifically, 17DMAG concentrations peaked at 30 min (9.0 ± 1.0 μg/g) and remained measurable (2.4 ± 0.6 μg/g) until 48 h after 17DMAG administration (the last time sampled, Table 1, Fig. 2b). The $AUC_{0-\infty}$ of 17DMAG in the tumor (19,876 μg/ml min) was approximately 19 times greater than the plasma 17DMAG AUC and was greater than that of any normal tissue except liver.

There was no evidence of 17AG or any other metabolite of 17DMAG present in plasma or any of the tissues.

Pharmacodynamic studies

The in vitro effect of 17DMAG on target proteins of logarithmically growing MDA-MB-231 cells was characterized before in vivo studies with MDA-MB-231 xenografts were undertaken. In vitro treatment of MDA-MB-231 cells with either vehicle or 20 n*M* 17DMAG had no effect on the relative protein concentration of HSP90, HSP70 or Raf-1 (data not shown); however, 24-h treatment with 100 n*M* 17DMAG resulted in a slight increase in HSP90, a greater than twofold increase in HSP70 and a 30% decrease in Raf-1 relative protein concentration compared to cells exposed only to vehicle (Fig. 3).

Treatment with vehicle did not alter the relative protein concentration of Raf-1, HSP90, or HSP70 in tumors, livers, kidneys, spleens, lungs, and hearts of mice killed at 5, 1,440 or 2880 min after vehicle administration (data not shown). Therefore, the relative protein concentration of these proteins in the 5-min vehicle-treated mice were used for comparison with their relative protein concentration in organs from 17DMAG-treated mice (Figs. 4, 5, 6).

At all times except 2 h, Raf-1 relative protein concentration in tumors of 17DMAG-treated mice were 20% less than the relative protein concentration of Raf-1 in tumors of vehicle-treated mice (Fig. 4). Both HSP90 and HSP70 were significantly decreased in tumors from mice treated with 17DMAG, although the magnitude and time course of these effects was quite different from that of Raf-1 (Fig. 4). At 2, 4, and 7 h after 17DMAG treatment, the relative protein concentration of HSP90 and HSP70 was between 40% and 50% of that in tumors from vehicle-treated mice. Between 24 h and 48 h after 17DMAG treatment, HSP90 and HSP70 concentrations in tumor increased so that by 48 h after 17DMAG treatment, they had returned to values similar to those observed in tumors of vehicle-treated mice.

17DMAG treatment also caused changes in Raf-1, HSP90 and HSP70 in normal murine tissues (Figs. 5 and 6). At all time points examined, relative protein concentration of Raf-1 in livers was decreased to 30–40% of that observed in the livers of vehicle-treated mice (Fig. 5). In contrast to tumors, there was no alteration in the hepatic relative protein concentration of HSP90 at any time after 17DMAG treatment. HSP70 was not detectable in the livers of vehicle-treated or untreated control mice. Therefore, the relative protein concentration of this protein in the livers of the 17DMAG-treated mice was determined as the ratio of the density of the HSP70 band to that of the β-actin band in the same sample; whereas 17DMAG treatment was associated with a decrease in tumor HSP70 relative protein concentration, 17DMAG administration was associated with an increase in HSP70 concentrations in liver, so that HSP70 relative protein concentration was easily detected in liver samples collected at 7, 24, and 48 h.

There were no changes in renal Raf-1 relative protein concentration at any of the time points examined after

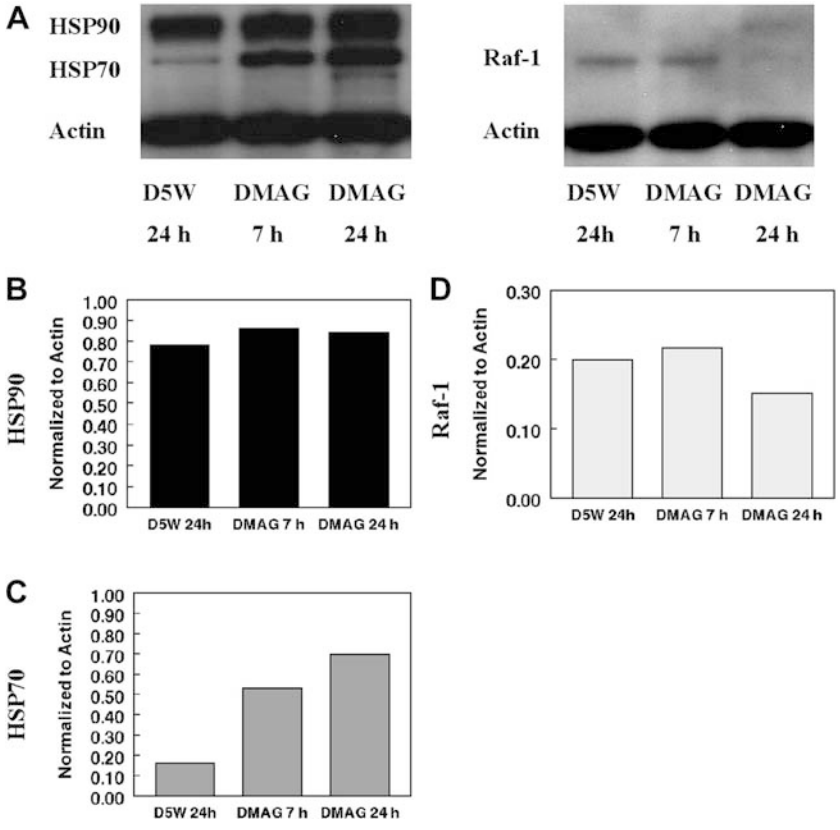

Fig. 3 Western blot analysis of Raf-1, HPS90, and HSP70 relative protein concentrations in MDA-MB-231 cells exposed to 100 n*M* 17DMAG in vitro. Results are representative of three experiments conducted using cells pooled from triplicate culture dishes after the addition of 17DMAG or vehicle. **a** Western blot imaging. **b**, **c**, **d** Changes in relative protein concentrations determined by densitometric measurements of the Western blots. Results are expressed as the ratio of target protein to actin, the control for sample loading

17DMAG administration (Fig. 6). Renal HSP90 relative protein concentration was decreased at 2 h and 4 h after 17DMAG treatment, but at 7 h and 24 h was similar to the relative protein concentration of HSP90 in the kidneys of the vehicle-treated mice. Renal HSP70 relative protein concentration was decreased at 2 h and 4 h after administration of 17DMAG, but at 7 h and 24 h had increased to approximately two times the relative protein concentration measured in the kidneys of vehicle-treated mice. 17DMAG treatment was not associated with any statistically significant changes in Raf-1, HSP90 or HSP70 relative protein concentrations in spleens, lungs, or hearts (data not shown).

Discussion

The benzoquinone ansamycin antibiotics, such as geldanamycin and herbimycin, possess potent antitumor activity [2, 11, 14, 27, 30, 32, 36, 39, 42, 52, 58, 60, 69], which is closely related to their ability to inhibit the function of the HSP90 molecular chaperone. By binding to the ATP-binding site of HSP90, geldanamycin blocks the proper folding and release of client signal transduction pathway molecules such as Raf-1, Erb-B2, Akt, and mutant p53 [2–5, 8, 9, 12, 31, 33, 34, 37, 39, 42, 43, 54, 56, 60, 65, 66, 68]. However, geldanamycin is poorly water-soluble and proved too toxic to be used clinically [63]. The geldanamycin analogue, 17AAG, is currently undergoing phase I clinical evaluation [7, 13, 24, 61, 67]. 17AAG downregulates the same oncoproteins as does geldanamycin, presumably through similar interactions with HSP90 [10, 28, 55, 58, 59]. 17DMAG, another geldanamycin analogue, is much more water-soluble than is 17AAG and is not metabolized to the potentially toxic metabolites that arise from CYP3A-mediated metabolism of the 17-allyl side chain of 17AAG [21, 18, 20].

The studies described here examined the relationship between the pharmacokinetics and the pharmacodynamic effects associated with administration of the highest nontoxic i.v. dose of 17DMAG to SCID mice bearing a human breast tumor xenograft. The plasma concentrations and distribution of 17DMAG in normal tissues of SCID mice bearing MDA-MB-231 xenografts were similar to those previously described in nontumor-bearing CD_2F_1 mice given the same i.v. dose of 17DMAG [21], although 17DMAG persisted somewhat longer in the tissues of SCID mice. In neither mouse strain was the metabolite 17AG detected in plasma or any tissue.

The retention of 17DMAG by tumor in this study is similar to that observed in earlier studies in which lower doses of 17AAG were administered to mice bearing PC3 human prostate cancer xenografts [19] or MDA-MB-453 human breast cancer xenografts [22]. These observations are quite consistent with recent observation that HSP90 derived from tumor cells has a 100-fold higher binding affinity for 17AAG than does HSP90 from normal cells [29].

In vitro treatment of MDA-MB-231 cells with 17DMAG doses comparable to the doses of 17AAG

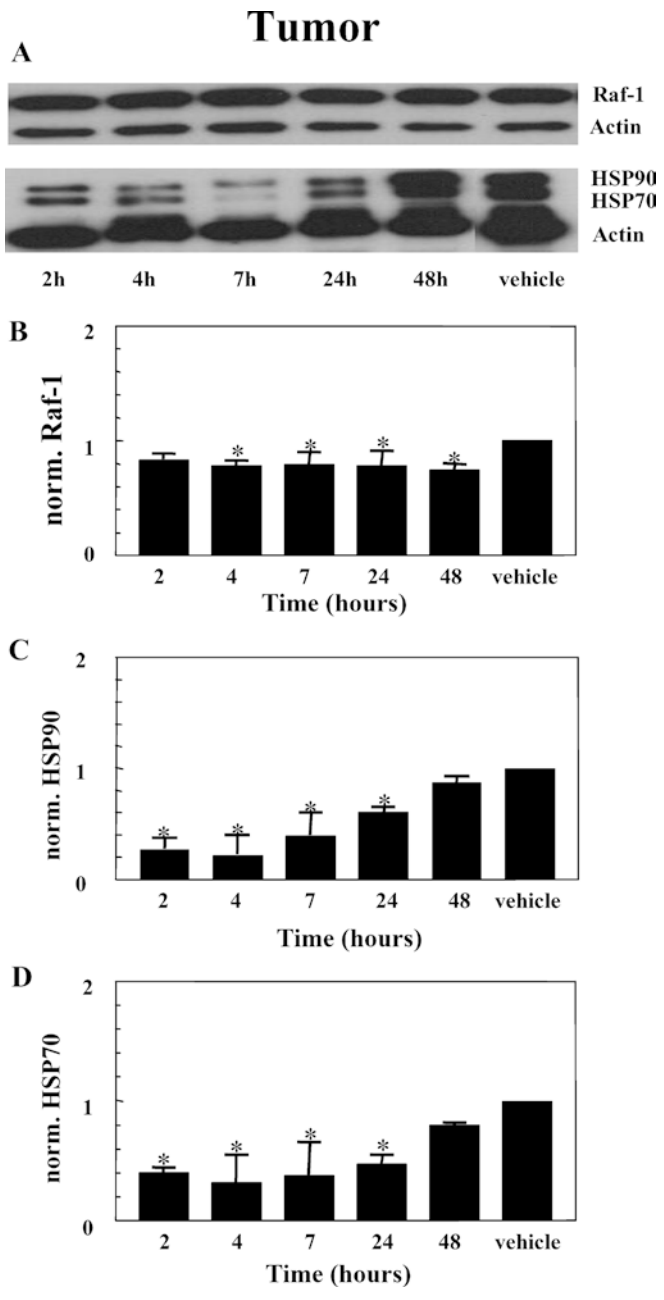

Fig. 4 Western blot analysis of Raf-1, HSP90, and HSP70 relative protein concentrations in the tumors of C.B-17 SCID mice bearing MDA-MB-231 tumors and treated with 75 mg/kg 17DMAG i.v. β-Actin served as a control for sample loading. **a** Western blot imaging. **b**, **c**, **d** Time courses of relative protein concentrations of target proteins in tumors to those in the tumors of vehicle-treated mice, as determined by densitometric measurements of tumors from three mice at each time point. The ratios of target proteins/actin were normalized to those of vehicle controls. Data are means $\pm$ SD. $^*P < 0.05$. **b** Raf-1; **c** HSP90; **d** HSP70

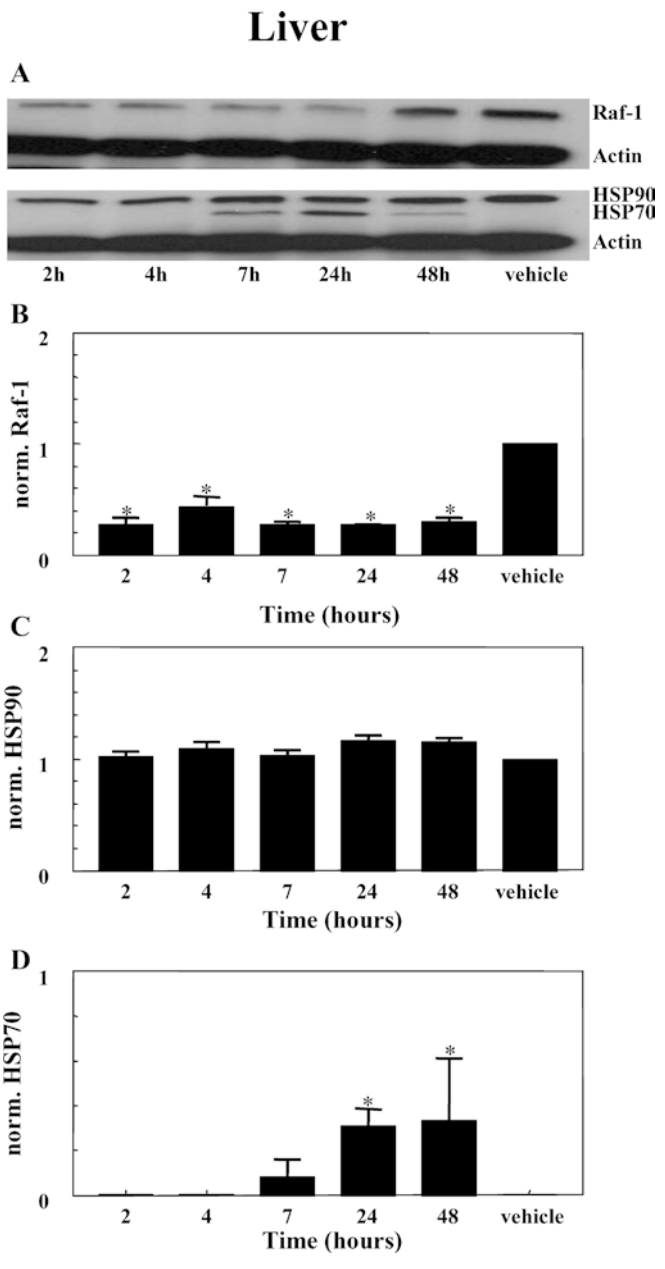

Fig. 5 Western blot analysis of Raf-1, HSP90, and HSP70 relative protein concentrations in the livers of C.B-17 SCID mice bearing MDA-MB-231 tumors and treated with 75 mg/kg 17DMAG i.v. β-Actin served as a control for sample loading. **a** Western blot imaging. **b**, **c** Time courses of relative protein concentrations of Raf-1 and HSP90 in livers from treated mice to those from livers of vehicle-treated mice. Relative protein concentrations were determined by densitometric measurements of livers from three mice at each time point. The ratios of target proteins/actin were normalized to those of vehicle controls. Data are means $\pm$ SD. $^*P < 0.05$. **d** Data represent the densitometric ratios of HSP70 at each time point to that of actin on the same lane. $^*P < 0.05$

required to alter relative protein concentrations of HSP90 client proteins [55] resulted in decreases in Raf-1 relative protein concentration and in increases in HSP70 relative protein concentration; however, the changes observed in cultured MDA-MB-231 cells after 17DMAG treatment were not the same as were observed in the xenografts following i.v. administration of 17DMAG. In the tumors, Raf-1 relative protein concentration was decreased by only 20%, while HSP70 was decreased in the tumors, in contrast to the relative protein concentration observed in vitro.

Although the ability of 17DMAG to modulate relative protein concentrations of HSP90 and its client

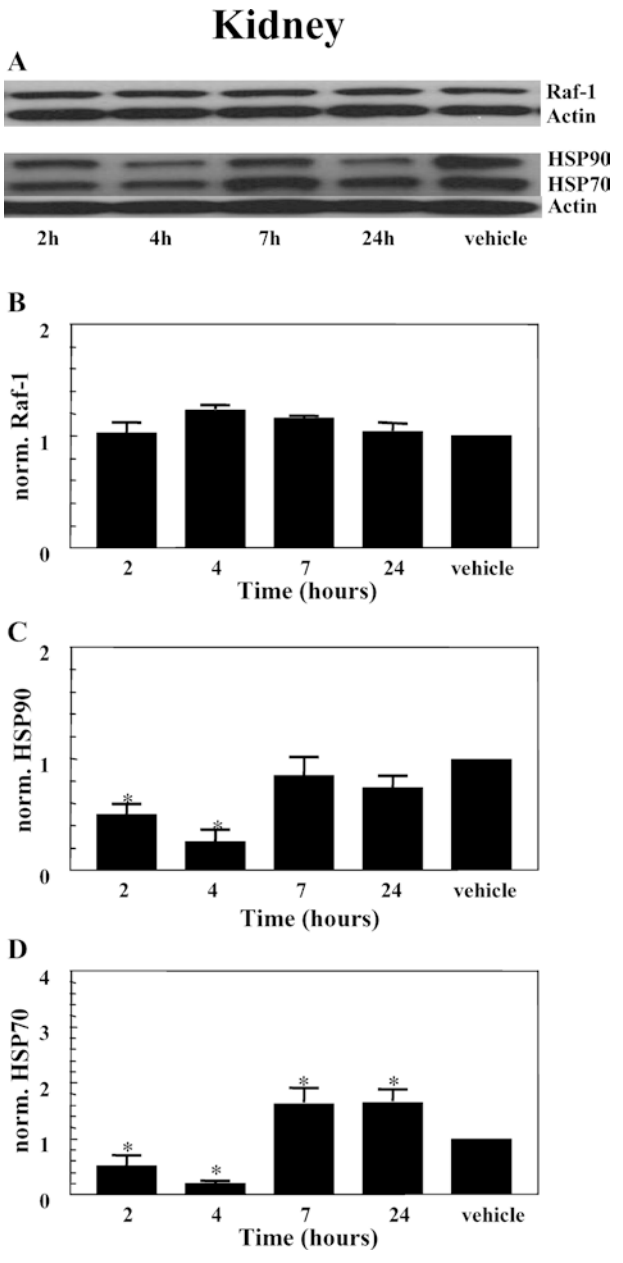

Fig. 6 Western blot analysis of Raf-1, HSP90, and HSP70 relative protein concentrations in the kidneys of C.B-17 SCID mice bearing MDA-MB-231 tumors and treated with 75 mg/kg 17DMAG i.v. β-Actin served as a control for sample loading. **a** Western blot imaging. **b**, **c**, **d** Time courses of relative concentration of target proteins in kidneys to those in the kidneys of vehicle-treated mice, as determined by densitometric measurements of kidneys from three mice at each time point. The ratios of target proteins/actin were normalized to those of vehicle controls. Data are means ± SD. **b** Raf-1; **c** HSP90; **d** HSP70

proteins in tumor tissue is consistent with changes in HSP90 client proteins described in preclinical and clinical studies with 17DMAG and 17AAG [6, 7, 19, 22, 59–61], it is unclear whether these changes correlate with antitumor effect. In mice bearing CWRSA6 xenografts, 4 days of treatment with 17AAG decreased intratumoral relative protein concentrations of HSP90 client proteins, including HER2, Akt, and the androgen receptor, and did so in a dose-dependent fashion [60]. In other studies, 17AAG treatment decreased HER2 and Raf-1 relative protein concentrations in MDA-MB-453 xenografts [22]. However, Banerji et al. found that HSP90 client proteins in two different ovarian xenografts were not affected in the same way following treatment with 17AAG [6]. Moreover, when the colon cell lines HT29, HCT116, KM12, and HCT15 were treated in vitro with 17AAG, the only consistent change observed in HSP90-related proteins was an increase in HSP70 [15]. This variability in the observed modulation of HSP90 client proteins by 17AAG and 17DMAG suggests that it will be a challenge to select informative pharmacodynamic markers that correlate with response as clinical development of these compounds progresses.

Although it is unclear as to what, if any, relationship exists between the pharmacokinetic and molecular pharmacodynamic effects of 17DMAG in tumor tissue and antitumor effect, analogous questions exist regarding how similar data in normal mouse tissues might relate to the toxicities associated with 17DMAG treatment. In view of the known hepatotoxicity of 17DMAG [23], it is interesting to note that the exposure of the liver to 17DMAG (25,693 μg/g min) was the highest among the normal tissues examined. Moreover, not only was liver the only normal tissue in which Raf-1 relative protein concentration decreased, but the decrease in hepatic Raf-1 relative protein concentration was greater than that observed in tumor tissue. On the other hand, hepatic Raf-1 relative protein concentration was unaffected by 17AAG treatment [22], yet 17AAG has proven to be hepatotoxic in preclinical and clinical studies [44, 46, 61, 67].

Understanding the basis of the antitumor activity of 17DMAG, as well as that of 17AAG, may be critical for their optimal evaluation and use in patients and for development of other novel HSP inhibitors. Although there are a growing number of studies on the potential anticancer mechanisms of HSP90-interactive drugs [4, 25, 35, 40, 41, 48, 53, 64], it is still unclear as to exactly how the molecular and cellular effects of 17AAG and 17DMAG result in suppression of tumor growth or clinical toxicities. This first report describes the in vivo effects of 17DMAG on signal transduction molecules that are HSP90 client proteins. The data indicate that 17DMAG acts in the same way as does 17AAG, with HSP90 as a molecular target and the potential inhibition of signaling through the Ras/Raf/MEK/ERK pathway. The complexity of the response at the cellular and molecular level makes it difficult to predict how generally applicable these observations are to different tumor types. Studies have demonstrated that 17AAG can deplete Raf-1 in ovarian, breast, and colon cancer cell lines [22, 27, 38, 57]. It is likely that many of the proteins, depleted by 17AAG, will also be affected by 17DMAG. However, the effect of this depletion on events downstream from the depleted protein will depend on how reliant the particular cell is on the pro-

teins that are depleted and also on the relative protein concentration profile of cell cycle control and pro- and antiapoptotic proteins within the cell. Despite the potential complexities of the pharmacology of 17DMAG, we have shown in these studies for the first time that HSP90 client proteins are affected by the drug in mice bearing human breast cancer xenografts. These results suggest that 17DMAG may allow exploitation of a new strategy for cancer treatment and may have fewer problems with solubility and toxicity than do its predecessors, geldanamycin and 17AAG.

Acknowledgements We thank Diane Mazzei and her colleagues in the University of Pittsburgh Animal Facility; without their expert assistance, these studies would not have been possible. We also thank Mr Ezekiel Woods for excellent secretarial assistance and the UPCI Hematology/Oncology Writing Group for constructive suggestions regarding the manuscript.

References

1. Akaike A (1979) A bayesian extention of the minimal AIC procedures of autoregressive model fitting. Biometrika 66:237
2. An WG, Schnur RC, Neckers L, Blagosklonny MV (1997) Depletion of p185erbB2, Raf-1 and mutant p53 proteins by geldanamycin derivatives correlates with antiproliferative activity. Cancer Chemother Pharmacol 40:60
3. An WG, Schulte TW, Neckers LM (2000) The heat shock protein 90 antagonist geldanamycin alters chaperone association with p210bcr-abl and v-src proteins before their degradation by the proteasome. Cell Growth Differ 11:355
4. Bagatell R, Khan O, Paine-Murrieta G, Taylor CW, Akinaga S, Whitesell L (2001) Destabilization of steroid receptors by heat shock protein 90-binding drugs: a ligand-independent approach to hormonal therapy of breast cancer. Clin Cancer Res 7:2076
5. Bamberger CM, Wald M, Bamberger AM, Schulte HM (1997) Inhibition of mineralocorticoid and glucocorticoid receptor function by the heat shock protein 90-binding agent geldanamycin. Mol Cell Endocrinol 131:233
6. Banerji U, Walton MI, Orr R, Kelland L, Judson IR, Workman P (2000) Development and validation of pharmacodynamic end points in tumor and normal tissue to assess the effect of the HSP90 molecular chaperone inhibitor 17-allylamino-17-demethoxy geldanamycin (17AAG). Proc Am Assoc Cancer Res 41:721a
7. Banerji U, O'Donnel A, Scurr M, Benson C, Stapleton S, Raynaud F, Clarke S, T1urner A, Workman P, Judson I (2003) A pharmacokinetically (PK)–pharmacodynamically (PD) guided phase I trial of the heat shock protein 90 (HSP90) inhibitor 17-allylamino,17-demethoxydgeldanamycin (17AAG). Proc Am Soc Clin Oncol 22:199
8. Basso AD, Solit DB, Munster PN, Rosen N (2002) Ansamycin antibiotics inhibit Akt activation and cyclin D expression in breast cancer cells that overexpress HER2. Oncogene 21:1159
9. Blagosklonny MV (2002) Hsp-90-associated oncoproteins: multiple targets of geldanamycin and its analogs. Leukemia 16:455
10. Blagosklonny MV, Toretsky J, Bohen S, Neckers L (1996) Mutant conformation of p53 translated in vitro or in vivo requires functional HSP90. Proc Natl Acad Sci U S A 93:8379
11. Brunton VG, Steele G, Lewis AD, Workman P (1998) Geldanamycin-induced cytotoxicity in human colon-cancer cell lines: evidence against the involvement of c-Src or DT-diaphorase. Cancer Chemother Pharmacol 41:417
12. Chen HS, Singh SS, Perdew GH (1997) The Ah receptor is a sensitive target of geldanamycin-induced protein turnover. Arch Biochem Biophys 348:190
13. Chen EX, Bies R, Ramanthan RK, Zuhowski EG, Trump DL, Egorin MJ (2002) Population pharmacokinetic (PK) analysis of 17-(allylamino)-17-demethoxygeldanamycin (AAG) in adult patients with advanced solid tumors. Proc Am Soc Clin Oncol 484:122a
14. Chiosis G, Timaul MN, Lucas B, Munster PN, Zheng FF, Sepp-Lorenzino L, Rosen N (2001) A small molecule designed to bind to the adenine nucleotide pocket of Hsp90 causes Her2 degradation and the growth arrest and differentiation of breast cancer cells. Chem Biol 8:289
15. Clarke PA, Hostein I, Banerji U, Stefano FD, Maloney A, Walton M, Judson I, Workman P (2000) Gene expression profiling of human colon cancer cells following inhibition of signal transduction by 17-allylamino-17-demethoxygeldanamycin, an inhibitor of the hsp90 molecular chaperone. Oncogene 19:4125
16. D'Argenio DZ, Schumitzky A (1979) A program package for simulation and parameter estimation in pharmacokinetic systems. Comput Programs Biomed 9:115
17. DeBoer C, Meulman PA, Wnuk RJ, Peterson DH (1970) Geldanamycin, a new antibiotic. J Antibiot (Tokyo) 23:442
18. Egorin MJ, Rosen DM, Wolff JH, Callery PS, Musser SM, Eiseman JL (1998) Metabolism of 17-(allylamino)-17-demethoxygeldanamycin (NSC 330507) by murine and human hepatic preparations. Cancer Res 58:2385
19. Egorin MJ, Sentz DL, Zuhowski EG, Dobson JM, Schulte TW, Neckers LM, Eiseman JL (1999) PC3 human prostrate xenograft retention of, and oncoprotein modulation by, 17-allylaminogeldanamycin (17AAG) in vivo. Proc Am Assoc Cancer Res 40:517
20. Egorin MJ, Zuhowski EG, Rosen DM, Sentz DL, Covey JM, Eiseman JL (2001) Plasma pharmacokinetics and tissue distribution of 17-(allylamino)-17-demethoxygeldanamycin (NSC 330507) in CD2F1 mice1. Cancer Chemother Pharmacol 47:291
21. Egorin MJ, Lagattuta TF, Hamburger DR, Covey JM, White KD, Musser SM, Eiseman JL (2002) Pharmacokinetics, tissue distribution, and metabolism of 17-(dimethylaminoethylamino)-17-demethoxygeldanamycin (NSC 707545) in CD2F1 mice and Fischer 344 rats. Cancer Chemother Pharmacol 49:7
22. Eiseman JL, Grimm A, Sentz DL, Lessor T, Gessner R, Zuhowski EG, Nemieboka N, Egorin MJ, Hamburger A (1999) Pharmacokinetics of 17-allylamino (17-demethoxy) geldanamycin in SCID mice bearing MDA-MB-453 xenografts and alterations in the expression of $p185^{Erb\text{-}B2}$ in the xenografts following treatment. Cancer Res 5(Suppl):3837
23. Glaze ER, Smith AC, Johnson DW, McCormick DL, Brown AB, Levin BS, Krishnaraj R, Lyubimov A, Egorin MJ, Tomaszewski JE (2003) Dose range-finding toxicity studies of 17-DMAG. Proc Am Assoc Cancer Res 44:162
24. Goetz M, Toft J, Reid J, Sloan J, Atherton P, Adjei A, Croghan G, Weinshilboum R, Erlichman C, Ames M (2002) A phase I trial of 17-allyl-amino-geldanamycin (17-AAG) in patients with advanced cancer. Euro J Cancer 38:54
25. Goetz MP, Toft DO, Ames MM, Erlichman C (2003) The Hsp90 chaperone complex as a novel target for cancer therapy. Anal Oncol 14:1169
26. Grenert JP, Sullivan WP, Fadden P, Haystead TA, Clark J, Mimnaugh E, Krutzsch H, Ochel HJ, Schulte TW, Sausville E, Neckers LM, Toft DO (1997) The amino-terminal domain of heat shock protein 90 (hsp90) that binds geldanamycin is an ATP/ADP switch domain that regulates hsp90 conformation. J Biol Chem 272:23843
27. Hostein I, Robertson D, DiStefano F, Workman P, Clarke PA (2001) Inhibition of signal transduction by the Hsp90 inhibitor 17-allylamino-17-demethoxygeldanamycin results in cytostasis and apoptosis. Cancer Res 61:4003
28. Jez JM, Chen JC, Rastelli G, Stroud RM, Santi DV (2003) Crystal structure and molecular modeling of 17-DMAG in complex with human Hsp90. Chem Biol 10:361
29. Kamal A, Thao L, Sensintaffar J, Zhang L, Boehm MF, Fritz LC, Burrows FJ (2003) A high-affinity conformation of Hsp90 confers tumour selectivity on Hsp90 inhibitors. Nature 425:407

30. Kelland LR, Sharp SY, Rogers PM, Myers TG, Workman P (1999) DT-Diaphorase expression and tumor cell sensitivity to 17-allylamino, 17-demethoxygeldanamycin, an inhibitor of heat shock protein 90. J Natl Cancer Inst 91:1940
31. Kim S, Kang J, Hu W, Evers BM, Chung DH (2003) Geldanamycin decreases Raf-1 and Akt levels and induces apoptosis in neuroblastomas. Int J Cancer 103:352
32. Kim S, Kang J, Qiao J, Kamal A, Burrows FJ, Evers BM, Chung DH (2003) Heat shock protein 90 inhibitors reduce neuroblastoma growth in vivo. Proc Am Assoc Cancer Res 44:152
33. Lavictoire SJ, Parolin DA, Klimowicz AC, Kelly JF, Lorimer IA (2003) Interaction of Hsp90 with the nascent form of the mutant epidermal growth factor receptor EGFRvIII. J Biol Chem 278:5292
34. Mabjeesh NJ, Post DE, Willard MT, Kaur B, Van Meir EG, Simons JW, Zhong H (2002) Geldanamycin induces degradation of hypoxia-inducible factor 1alpha protein via the proteosome pathway in prostate cancer cells. Cancer Res 62:2478
35. Maloney A, Workman P (2002) HSP90 as a new therapeutic target for cancer therapy: the story unfolds. Expert Opin Biol Ther 2:3
36. Mandler R, Wu C, Sausville EA, Roettinger AJ, Newman DJ, Ho DK, King CR, Yang D, Lippman ME, Landolfi NF, Dadachova E, Brechbiel MW, Waldmann TA (2000) Immunoconjugates of geldanamycin and anti-HER2 monoclonal antibodies: antiproliferative activity on human breast carcinoma cell lines. J Natl Cancer Inst 92:1573
37. Miller P, DiOrio C, Moyer M, Schnur RC, Bruskin A, Cullen W, Moyer JD (1994) Depletion of the erbB-2 gene product p185 by benzoquinoid ansamycins. Cancer Res 54:2724
38. Munster PN, Basso A, Solit D, Norton L, Rosen N (2001) Modulation of Hsp90 function by ansamycins sensitizes breast cancer cells to chemotherapy-induced apoptosis in an RB- and schedule-dependent manner. See: E.A. Sausville, Combining cytotoxics and 17-allylamino, 17-demethoxygeldanamycin: sequence and tumor biology matters, Clin. Cancer Res., 7: 2155–2158, 2001. Clin Cancer Res 7:2228
39. Munster PN, Marchion DC, Basso AD, Rosen N (2002) Degradation of HER2 by ansamycins induces growth arrest and apoptosis in cells with HER2 overexpression via a HER3, phosphatidylinositol 3'-kinase-AKT-dependent pathway. Cancer Res 62:3132
40. Neckers L (2002) Hsp90 inhibitors as novel cancer chemotherapeutic agents. Trends Mol Med 8:S55–S61
41. Nimmanapalli R, Bhalla K (2002) Novel targeted therapies for Bcr-Abl positive acute leukemias: beyond STI571. Oncogene 21:8584
42. Nimmanapalli R, O'Bryan E, Bhalla K (2001) Geldanamycin and its analogue 17-allylamino-17-demethoxygeldanamycin lowers Bcr-Abl levels and induces apoptosis and differentiation of Bcr-Abl-positive human leukemic blasts. Cancer Res 61:1799
43. Nimmanapalli R, O'Bryan E, Kuhn D, Yamaguchi H, Wang HG, Bhalla KN (2003) Regulation of 17-AAG-induced apoptosis: role of Bcl-2, Bcl-XL, and Bax downstream of 17-AAG-mediated down-regulation of Akt, Raf-1, and Src kinases. Blood 102:269
44. Noker PE, Thompson RB, Smith AC, Tomaszewski JE, Page JG (1999) Toxicity and pharmacokinetics of 17-allylaminogeldanamycin (17-AAG, NSC-330507) in dogs. Proc Am Assoc Cancer Res 40:121
45. Obermann WM, Sondermann H, Russo AA, Pavletich NP, Hartl FU (1998) In vivo function of Hsp90 is dependent on ATP binding and ATP hydrolysis. J Cell Biol 143:901
46. Page JG, Noker PE, Tomaszewski JE, Smith AC (1999) Lack of schedule dependent toxicity of 17-allylaminogeldanamycin (17-AAG, NSC-330507) in rats. Proc Am Assoc Cancer Res 40:121
47. Panaretou B, Prodromou C, Roe SM, O'Brien R, Ladbury JE, Piper PW, Pearl LH (1998) ATP binding and hydrolysis are essential to the function of the Hsp90 molecular chaperone in vivo. EMBO J 17:4829
48. Piper PW (2001) The Hsp90 chaperone as a promising drug target. Curr Opin Investig Drugs 2:1606
49. Prodromou C, Roe SM, O'Brien R, Ladbury JE, Piper PW, Pearl LH (1997) Identification and structural characterization of the ATP/ADP-binding site in the Hsp90 molecular chaperone. Cell 90:65
50. Rocci ML Jr, Jusko WJ (1983) LAGRAN program for area and moments in pharmacokinetic analysis. Comput Programs Biomed 16:203
51. Roe SM, Prodromou C, O'Brien R, Ladbury JE, Piper PW, Pearl LH (1999) Structural basis for inhibition of the Hsp90 molecular chaperone by the antitumor antibiotics radicicol and geldanamycin. J Med Chem 42:260
52. Sasaki K, Yasuda H, Onodera K (1979) Growth inhibition of virus transformed cells in vitro and antitumor activity in vivo of geldanamycin and its derivatives. J Antibiot (Tokyo) 32:849
53. Scheibel T, Buchner J (1998) The Hsp90 complex—a supercharperone machine as a novel drug target. Biochem Pharmacol 56:675
54. Schnur RC, Corman ML, Gallaschun RJ, Cooper BA, Dee MF, Doty JL, Muzzi ML, Moyer JD, DiOrio CI, Barbacci EG (1995) Inhibition of the oncogene product p185erbB-2 in vitro and in vivo by geldanamycin and dihydrogeldanamycin derivatives. J Med Chem 38:3806
55. Schulte TW, Neckers LM (1998) The benzoquinone ansamycin 17-allylamino-17-demethoxygeldanamycin binds to HSP90 and shares important biologic activities with geldanamycin. Cancer Chemother Pharmacol 42:273
56. Schulte TW, Blagosklonny MV, Romanova L, Mushinski JF, Monia BP, Johnston JF, Nguyen P, Trepel J, Neckers LM (1996) Destabilization of Raf-1 by geldanamycin leads to disruption of the Raf-1-MEK-mitogen-activated protein kinase signalling pathway. Mol Cell Biol 16:5839
57. Smith V, Hobbs S, Court W, Eccles S, Workman P, Kelland LR (2002) ErbB2 overexpression in an ovarian cancer cell line confers sensitivity to the HSP90 inhibitor geldanamycin. Anticancer Res 22:1993
58. Smith V, Sausville EA, Camalier RF, Fiebig HH, Burger AM (2002) 17-DMAG (NSC 07545), a water-soluble geldanamycin analog, has superior in vitro and in vivo antitumor activity compared to the hsp90 inhibitor 17-AAG. Eur J Cancer 38 [Suppl 7]:60
59. Smith V, Sausville EA, Camalier RF, Fiebig HH, Burger AM (2003) 17-DMA-geldanamycin is a novel water-soluble, orally bioavailable Hsp90 inhibitor with potent in vitro and in vivo anticancer activity. Proc Am Assoc Cancer Res 44:153
60. Solit DB, Zheng FF, Drobnjak M, Munster PN, Higgins B, Verbel D, Heller G, Tong W, Cordon-Cardo C, Agus DB, Scher HI, Rosen N (2002) 17-Allylamino-17-demethoxygeldanamycin induces the degradation of androgen receptor and HER-2/neu and inhibits the growth of prostate cancer xenografts. Clin Cancer Res 8:986
61. Solit DB, Anana M, Valentin G, De La Cruz A, Tong W, Busam K, Reuter V, Kelly WK, Rosen N, Scher H (2003) Phase I trial of 17-AAG (17-allylamino-17-demethoxygeldanamycin) in patients (pts) with advanced cancer. Proc Am Soc Clin Oncol 22:198
62. Stebbins CE, Russo AA, Schneider C, Rosen N, Hartl FU, Pavletich NP (1997) Crystal structure of an Hsp90-geldanamycin complex: targeting of a protein chaperone by an antitumor agent. Cell 89:239
63. Supko JG, Hickman RL, Grever MR, Malspeis L (1995) Preclinical pharmacologic evaluation of geldanamycin as an antitumor agent. Cancer Chemother Pharmacol 36:305
64. Takimoto CH, Diggikar S (2002) Heat shock protein and proteasome targeting agents. Hematol Oncol Clin North Am 16:1269

65. Uehara Y, Hori M, Takeuchi T, Umezawa H (1986) Phenotypic change from transformed to normal induced by benzoquinonoid ansamycins accompanies inactivation of p60src in rat kidney cells infected with Rous sarcoma virus. Mol Cell Biol 6:2198
66. Whitesell L, Sutphin PD, Pulcini EJ, Martinez JD, Cook PH (1998) The physical association of multiple molecular chaperone proteins with mutant p53 is altered by geldanamycin, an hsp90-binding agent. Mol Cell Biol 18:1517
67. Wilson RH, Takimoto CH, Agnew EB, Morrison G, Grollman F, Thomas RR, Saif MW, Hopkins J, Allegra C, Grochow L, Szabo E, Hamilton JM, Monahan BP, Neckers L, Grem JL (2001) Phase I pharmacologic study of 17-(allylamino)-17-demethoxygeldanamycin (AAG) in adult patients with advanced solid tumors. Proc Am Soc Clin Oncol 20:82a
68. Xu W, Mimnaugh E, Rosser MF, Nicchitta C, Marcu M, Yarden Y, Neckers L (2001) Sensitivity of mature Erbb2 to geldanamycin is conferred by its kinase domain and is mediated by the chaperone protein Hsp90. J Biol Chem 276:3702
69. Yamaki H, Suzuki H, Choi EC, Tanaka N (1982) Inhibition of DNA synthesis in murine tumor cells by geldanamycin, an antibiotic of the benzoquinoid ansamycin group. J Antibiot (Tokyo) 35:886
70. Yeh KC, Kwan KC (1978) A comparison of numerical integrating algorithms by trapezoidal, Lagrange, and spline approximation. J Pharmacokinet Biopharm 6:79